Supporting Information

Mn^{2+}-Intercalated Hydrated Vanadium Oxide with Tunable Spacing for High-Performance Zinc-Ion Batteries

Yuling Tu[a], Dejun Gong[a], Lirong Jia[a], Zeming Lu[a], Jun Gao[a], Hui Chai[a*], Yali Cao[a], Xiaogang Zhang[b], Naseem Iqbal[c]

[a]State Key Laboratory of Chemistry and Utilization of Carbon Based Energy Resources; Key Laboratory of Energy Materials Chemistry, Ministry of Education; Institute of Applied Chemistry, College of Chemistry, Xinjiang University, Urumqi, 830017, Xinjiang, PR China

[b]College of Material Science and Engineering, Nanjing University of Aeronautics and Astronautics, Yudao Street 29, Nanjing 210016, PR China

[c]US-Pakistan Centre for Advanced Studies in Energy, (USPCAS-E), National University of Sciences and Technology (NUST), H-12, Islamabad 44000, Pakistan

*Corresponding author: Tel: +86 9918583083; Fax: +86 9918588883; E-mail: huichmails@163.com

Material characterization

The crystalline structure of the synthesized material was examined by X-ray diffraction (XRD) using Cu Kα radiation (λ = 1.5406 Å). Diffraction patterns were recorded over a 2θ range of 5° to 80° at a scanning rate of 5° min^{-1}. Microstructural features were visualized using a Hitachi SU-4800 scanning electron microscope (SEM). To obtain more precise structural information and perform elemental distribution analysis, transmission electron microscopy (TEM) analysis was conducted utilizing a JEM-2100F microscope that was fitted with an X-Max80T energy-dispersive spectroscopy (EDS) detector. Thermal behavior was assessed via thermogravimetric analysis (TGA) on an SDT650 instrument coupled with a DSC300 module under a nitrogen environment. To characterize the textural properties of the sample (such as specific surface area and pore size distribution), we employed an ASAP 2460 analyzer to conduct low-temperature nitrogen adsorption experiments based on the BET theoretical method. Additionally, the Raman spectra of the samples were acquired using a HORIBA LabRAM HR Evolution spectrometer, and their

surface chemical states were analyzed via X-ray photoelectron spectroscopy (XPS) performed on a Thermo Fisher ESCALAB 250Xi system.

Electrochemical Measurements.

The electrochemical properties of the test material were evaluated using a CR2032 button cell. The active material, conductive carbon black, and polyvinylidene fluoride (PVDF) binder were combined in a mass ratio of 70:20:10. An adequate volume of N-methyl-2-pyrrolidone (NMP) was introduced, and the mixture was thoroughly ground to form a homogeneous slurry. This paste was applied to a stainless steel mesh current collector. The electrode was dried in a vacuum oven at 60°C for 12 h. Zinc foil served as the anode, with filter paper and 3 M $ZnSO_4$ acting as the cathode, separator, and electrolyte, respectively. The cathode material was loaded at a mass loading of 1.0-1.5 mg cm^{-2}. Subsequently, the cell was tested for rate performance, cycling stability, self-discharge, and GITT using a Blue Electrode System (CT3002A) within a voltage window of 0.2-1.6 V. Cyclic voltammetry (CV) and electrochemical impedance spectroscopy (EIS) were performed on the material using an electrochemical workstation (CHI 660E).

Figure

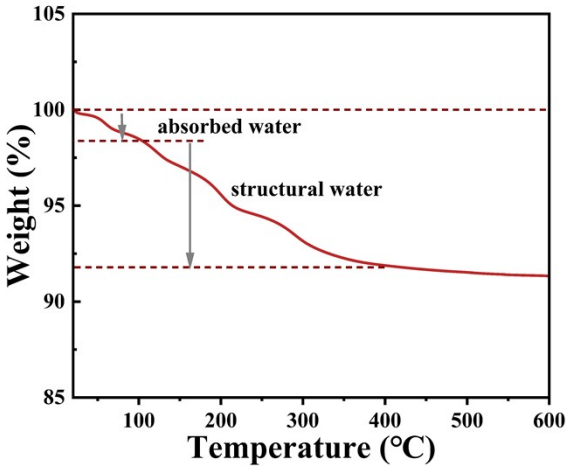

Figure S1. TGA curve of MVOH.

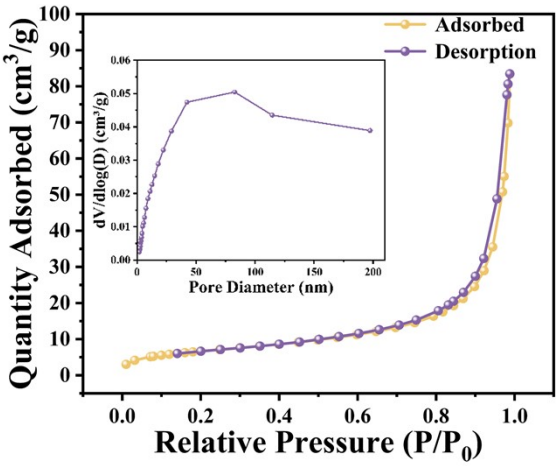

Figure S2. Nitrogen adsorption-desorption isotherms and pore size distribution of VOH.

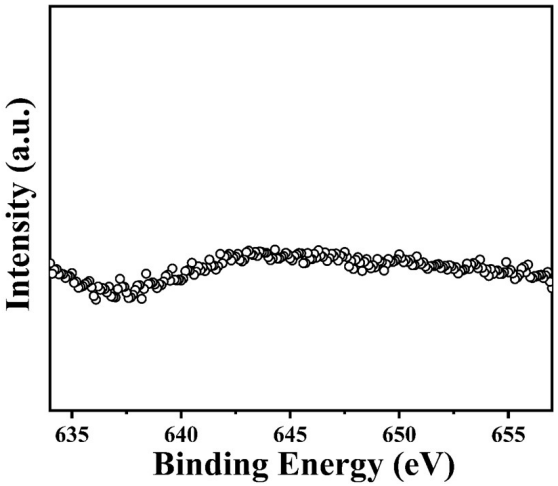

Figure S3. Mn 2p XPS spectrum of VOH.

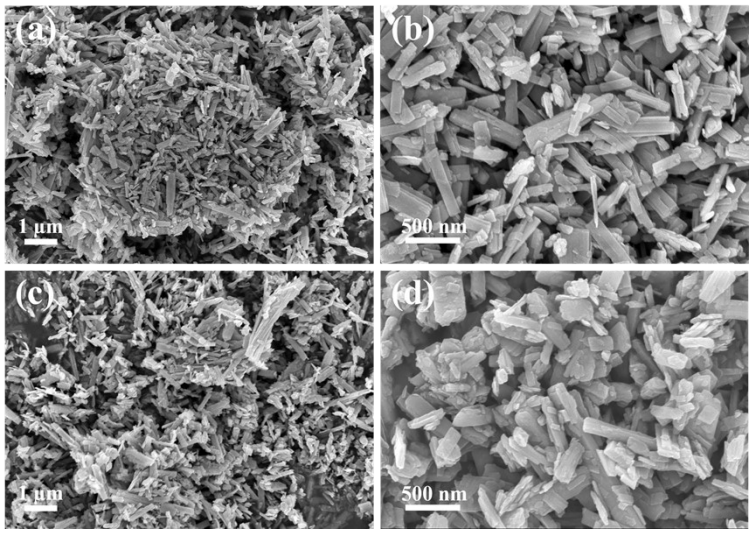

Figure S4. (a, b) SEM images of MVOH-1; (c, d) SEM images of MVOH-3.

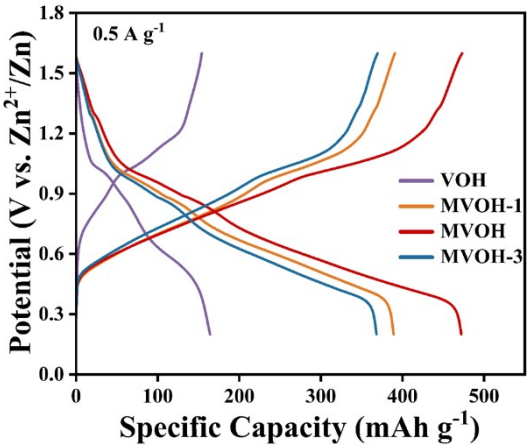

Figure S5. GCD curves for different materials at the same current density (0.5 A g^{-1}).

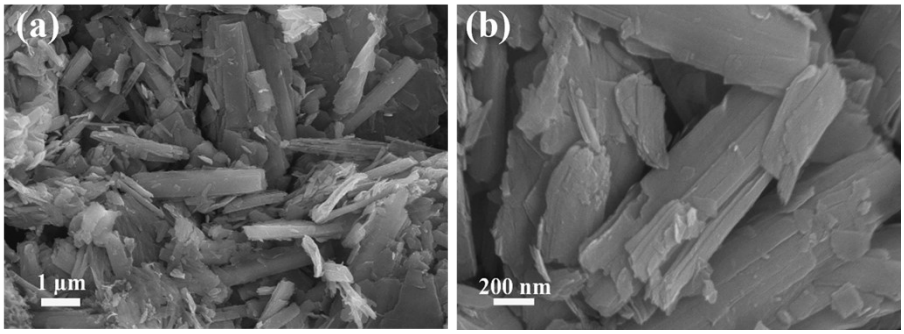

Figure S6. SEM image of MVOH after 3000 cycles at 5 A g^{-1}.

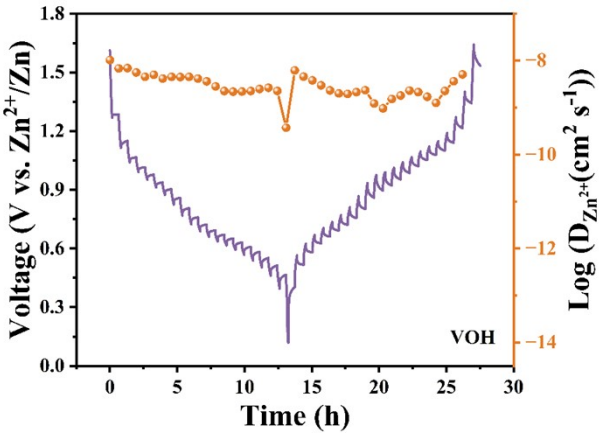

Figure S7. GITT curves and diffusion coefficients of VOH.

Table

Table S1. Element Content of the Sample

elements	sample element content *Wt* (%)
V	46.41
Mn	4.29

Table S2. Related References

Materials	Current density ($A\ g^{-1}$)	Capacity ($mAh\ g^{-1}$) / Number	Capacity retention rate	Ref.
MVOH	5	250.1 (3000)	80.1%	This work
VMO/rGO	5	228.3 (3000)	42%	[1]
V_2O_3@C	5	207 (2000)	78%	[2]
CNVO	5	183 (1300)	91%	[3]
NVO/PDAN	5	178.6 (2000)	77%	[4]
KVOH	1	290 (800)	76.7%	[5]
$Mn_2V_2O_7$	2	150 (2500)	/	[6]
HVO/GO-CNT	1	251.9 (1000)	82.6%	[7]
5-MoVOH	2	216.2 (1000)	95%	[8]
BNVO-3	5	109.8 (1500)	92.9%	[9]

Reference

1. Y. X. Luo, Q. Kuang, Y. B. Li, J. X. Zhan, Y. H. Cheng, Q. H. Fan, Y. Z. Dong and Y. M. Zhao, Decoupling Zn^{2+}/H^{+} co-insertion in $VOMo_4O$/rGO heterostructure for dendrite-free symmetric zinc-ion batteries, Chem Eng J, 2026, 532, 174457.
2. D. Q. Wang, W. H. Liang, X. D. He, Y. Yang, S. Wang, J. Li, J. C. Wang and H. L. Jin, V_2O_3@C Microspheres as the High-Performance Cathode Materials for Advanced Aqueous Zinc-Ion Storage, ACS Appl Mater Inter, 2023, 15, 20876-20884.

3. S. Yao, Y. G. Sun, Z. Cui and G. J. He, Ca doping $NH_4V_4O_{10}$ with enhanced zinc-ion storage ability and structural stability for high performance aqueous zinc-ion batteries, Rare Metals, 2025, 44, 6081-6091.
4. Y. Xu, X. Z. Tang, X. C. Xie, N. Wang and W. C. Hu, Construction of a hybrid layered composite with intercalated polymer as cathode for aqueous zinc ion batteries, J Colloid Interf Sci, 2025, 692, 137514.
5. J. A. Chen, X. J. Hou, X. L. Wang, C. X. Wang, J. W. Wen, Y. J. Bu, G. Y. Huang, T. T. Cao and S. M. Xu, Bi-intercalated vanadium pentoxide synthesized hydrogen peroxide-induced phase transition for highly stable cathode in aqueous zinc ion batteries, J Mater Chem A, 2024, 12, 11322-11331.
6. F. F. Mao, T. Yu, Y. W. Li, S. Q. Sheng, Q. Zhang and J. H. Yao, Single-crystalline $Mn_2V_2O_7$ with high operating voltage and energy density as a cathode material for aqueous zinc-ion batteries, J Energy Storage, 2025, 109, 115241.
7. D. W. Rao, W. W. Zhang, B. C. Cheng, Y. Wang, C. S. F. Lei, Q. Y. An, M. Huang and L. Q. Mai, $V_2O_5{\cdot}nH_2O$ and Graphene Oxide/CNTs Composite Film as Binder-Free Cathode for Aqueous Zinc-Ion Batteries, Batteries Supercaps, 2024, 7, 2400046.
8. G. F. Shi, P. Zhao, P. Gao, Y. Y. Xing and B. X. Shen, Employing the optimized pre-intercalation strategy to design functional Mo pre-intercalated hydrated vanadium oxide for aqueous zinc-ion batteries, J Energy Storage, 2024, 78, 110057.
9. Z. H. Deng, W. Shao, H. Y. Wang, Y. B. Wang, J. Sheng, H. C. Mu, C. Lian and W. J. Wu, Augmenting specific capacitance of ammonium vanadate cathode in aqueous zinc-ion batteries via barium doping directed by glutamic acid, J Power Sources, 2024, 614, 234976.